

Multiresponse Kinetic Modeling of Acrylamide Formation in Low Moisture Food Systems Like Nuts and Seeds during Roasting

Dilara Şen and Vural Gökmen*

Cite This: *ACS Food Sci. Technol.* 2023, 3, 1606–1616

Read Online

ACCESS |



Metrics & More



Article Recommendations



Supporting Information

ABSTRACT: This study aimed to propose a kinetic model by using the multiresponse kinetic modeling approach for acrylamide formation in low-moisture foods at around neutral pH with a restricted amount of reducing sugar content but rich in sucrose and free amino acids. Four types of edible nuts and seeds were roasted at 160, 180, and 200 °C for 5 to 60 min to represent these dry systems. The changes in the concentrations of reactants and products of acrylamide formation were monitored during roasting. According to the proposed model, sucrose degraded to glucose and fructofuranosyl cation; 5-hydroxymethylfurfural was mainly formed through the 3-deoxyglucosone pathway in all samples at 160 and 180 °C; and the reaction of asparagine with 5-hydroxymethylfurfural was confirmed as the predominant pathway for acrylamide formation. This proposed model also helps to determine the acrylamide concentration formed during the roasting of foods that have similar compositional characteristics with samples in this study.

KEYWORDS: roasting, nuts and seeds, Maillard reaction, acrylamide, 5-hydroxymethylfurfural, multiresponse kinetic modeling

INTRODUCTION

The consumption of nuts and seeds is considered a part of a healthy diet due to their vitamin, mineral, dietary fiber, polyphenol, and high unsaturated fatty acid content.¹ Besides being used as an ingredient in bakery and confectionery products, they can also be consumed raw or after being roasted as snacks. The roasting process, which is generally performed at 130–180 °C for periods depending on the product or temperature, improves the organoleptic properties of nuts and seeds by inducing the development of desirable taste, aroma, texture, and color. Apart from these favorable consequences, the thermal process can also cause potentially adverse health effects by promoting the formation of potentially toxic or carcinogenic compounds.

One of the undesired compounds, acrylamide (ACR), has been classified as a potential human carcinogen by the International Agency for Research on Cancer.² The major route for ACR formation is thermal degradation of asparagine in the presence of reducing sugars. The decarboxylated Amadori product (AP) of asparagine with reducing sugars was reported to be the direct precursor of ACR.³ There are many studies on ACR formation both in model studies and in real foods, especially those containing a high amount of protein and carbohydrates. It is known that for the Maillard reaction the water content is an important factor, and reducing sugars are the primary reactants. Although nuts and seeds seem to be unfavorable due to their restricted amount of reducing sugar and low moisture content, their available amounts of sucrose and asparagine content make them a suitable medium for ACR formation. Therefore, a considerable amount of ACR is inevitable in many nuts and seeds.⁴

Another heat induced neo-formed compound, 5-hydroxymethylfurfural (HMF), is formed mainly through the Maillard

reaction or sugar degradation.⁵ Its conversion to sulfoxymethylfurfural, which is reported to be a genotoxic and nephrotoxic compound, makes HMF responsible for negative health effects. HMF can also be used as a quality indicator for heat load in thermally processed foods.⁶

Moisture content or water activity is one of the important factors that affects the rate of Maillard reaction. Increasing the water activity to a certain extent increases the solubility and diffusion of the reactants and, thus, the reaction rates. However, at low water content, melting provides reactivity to reactants instead of diffusion, and dehydration reactions become predominant instead of hydrolysis reactions.^{7,8} Therefore, it is inappropriate to explain the ACR formation mechanism in low-moisture food systems with kinetic models based on model solutions and aqueous food matrices.

Multiresponse kinetic modeling of reactions can be used as a powerful tool to understand complex reaction mechanisms and obtain better insight into the whole mechanism. In this way, rate-determining steps can be determined and the link between reactants and products can be expressed quantitatively.^{9,10}

In previous studies, kinetic modeling of the acrylamide formation that occurs during the roasting process was carried out in coffee and sesame samples, which are prominent with their sucrose composition and low moisture content.^{11,12} The aim of this study is to propose a generic model expressing acrylamide formation that will be valid in such food systems in

Received: August 9, 2023

Revised: August 16, 2023

Accepted: August 23, 2023

Published: September 4, 2023



order to better understand the role of sucrose decomposition and HMF formation in acrylamide formation in nuts and seeds, which are widely consumed in the roasted form.

In this study, the ACR formation mechanism was investigated during the roasting of sucrose-rich low moisture foods. Sunflower (*Helianthus annuus* L.), flaxseed also known as linseed (*Linum usitatissimum* L.), peanut (*Arachis hypogaea* L.), and almond (*Prunus dulcis*) were studied to represent the nuts and seeds. The concentrations of reactants and products were monitored during the roasting of these samples, and a kinetic model was revealed by using the multiresponse kinetic modeling approach. It was aimed to build a simple model that will be suitable for a wide range of roasted foods, which have a similar composition to the examples studied here. This simple model might also enable us to develop mitigation strategies for controlling the formation of ACR.

MATERIALS AND METHODS

Chemicals and Consumables. High purity (>99%) D-sucrose, D-glucose, and D-fructose were obtained from Sigma-Aldrich (Dienhofen, Germany). All amino acids (>98%) were purchased from Merck Co. (Darmstadt, Germany). Methanol and acetonitrile were obtained from Merck (Darmstadt, Germany). Formic acid (98%) was obtained from JT Baker (Deventer, Holland). Potassium hexacyanoferrate, zinc sulfate, disodium hydrogen phosphate anhydrous, and sodium dihydrogen phosphate dihydrate were purchased from Merck (Darmstadt, Germany). The Carrez I and Carrez II solutions were prepared by dissolving 15 g of potassium hexacyanoferrate and 30 g of zinc sulfate in 100 mL of water, respectively. 3-Deoxyglucosone (75%), *o*-phenylenediamine (98%), and diethylenetriaminepentaacetic acid (DETAPAC) (98%) were purchased from Sigma-Aldrich (Steinheim, Germany). 5-Hydroxymethylfurfural (98%) was purchased from Acros (Geel, Belgium). Syringe filters (nylon, 0.45 μm), Oasis HLB, and MCX cartridges (30 mg, 1 mL) were supplied by Waters (Millford, MA). Deionized water (0.055 $\mu\text{S}/\text{cm}$) was used throughout the experiments.

Roasting and Extraction of Samples. Raw sunflower seed, peanut, almond, and flaxseed samples were purchased from a local market (Ankara, Turkey). As previously described by us elsewhere, a 30 g portion of the sample was placed on an aluminum plate and roasted in a conventional oven (Memmert UN 55, Germany) at 160, 180, and 200 °C for 3 to 60 min.¹³ Roasting conditions were selected to include both industrial and extreme conditions. Roasted samples were ground and kept frozen at -18 °C prior to analysis. The roasting treatments were performed in triplicate for each nut and seed at each time-temperature combination.

Triple stage extraction was performed for 1 g of ground sample by using 20 mL of water (10, 5, 5 mL) according to the procedure described before.¹⁴ The samples were weighed into tubes, and for each extraction step, after the addition of water, the mixture was vortexed for 5 min, and tubes were stored at -18 °C for 5 min to obtain a clear extract prior to centrifuging at 8000 \times g for 5 min. Supernatants were collected in another tube and centrifuged at 8000 \times g for 5 min.

Analysis of Sugars. One mL of aqueous extract was precipitated by Carrez clarification by mixing 50 μL of Carrez I and 50 μL of Carrez II followed by vortexing for 3 min and centrifugation at 12000 \times g for 5 min. The supernatant was passed through the HLB cartridge and preconditioned with 1 mL of methanol and 1 mL of water, subsequently. The first 8 drops were discarded, and the rest was collected into a vial. Analysis of sugars was performed as described by Kocadağı and Gökmen⁷ on Agilent 1200 HPLC system coupled with a refractive index detector (RID), a quaternary pump, an autosampler, and a column oven. Shodex Sugar SH-1011 column (300 mm \times 8 mm i.d., 6 μm) (Tokyo, Japan) conditioned to 50 °C was used for chromatographic separation. An isocratic elution of 0.01 N H₂SO₄ in water (v/v) at a flow rate of 1 mL/min was used. The injection volume was 5 μL . The concentrations of sucrose, glucose, and

fructose were calculated according to calibration curves built between the concentrations of 0.1 and 1 g/100 mL. The limit of detection (LOD) and limit of quantitation (LOQ) values for sugars were from 0.001 to 0.004 g/100 g and from 0.005 to 0.015 g/100 g, respectively.

Analysis of Free Amino Acids. The analysis of free amino acids was carried out according to the method described by Hamzalıoğlu and Gökmen.¹² One mL of previously prepared aqueous extracts was mixed with an equal volume of acetonitrile and centrifuged at 10000 \times g for 5 min. The supernatant was filtered through a 0.45 μm nylon filter and collected in an autosampler vial. Free amino acids were determined by Agilent Ultivo Triple Quadrupole MS coupled to Agilent 1260 HPLC in positive mode. Chromatographic separations were performed on a Sequant-ZIC-HILIC (250 \times 4.6 mm i.d., 5 μm) column at 30 °C. A gradient mixture of (A) 0.1% formic acid in water and (B) 0.1% formic acid in acetonitrile was used as a mobile phase at a flow rate of 0.5 mL/min. The eluent composition starting from 20% A was conditioned for 3 min, then increased to 60% A in 2 min, and held for 3 min. Then it linearly decreased to 20% A in 1 min and remained there for 3 min. The total chromatographic run was completed in 12 min. The electrospray source had the following settings: capillary voltage of 1.5 kV; nozzle voltage of 500 V; nebulizer pressure of 40 psi; gas (nitrogen) temperature at 300 °C with a flow rate of 10 L/min; and sheath gas temperature at 375 °C with a flow rate of 12 L/min. Multiple reaction monitoring (MRM) of two channels was used to identify amino acids, and both the product and precursor ions were monitored. MRM transitions used to detect individual free amino acids were stated in Table S1. Quantification was performed by means of external calibration curves built for all amino acids in a range between 1 and 100 $\mu\text{mol}/\text{L}$. The LOD and LOQ values for free amino acids were from 0.03 to 0.16 mg/kg and from 0.11 to 0.54 mg/kg based on signal-to-noise ratios of 3 and 10, respectively.

Analysis of Acrylamide. One mL of aqueous extract was passed through the preconditioned Oasis MCX cartridge to remove interfering compounds before HPLC analysis. The cartridge was preconditioned by passing 1 mL of methanol and 1 mL of water, subsequently. The first 8 drops of eluent were discarded, and the rest were collected into a vial. ACR content of samples was analyzed by Agilent Ultivo Triple Quadrupole MS coupled to Agilent 1260 HPLC in positive mode. The sample was injected into an Atlantis T3 column (150 mm \times 4.6 mm i.d., 3 μm) and conditioned to 40 °C. 10 mM formic acid in water was used as a mobile phase with a flow rate of 0.5 mL/min. MS system had the following interface parameters: sheath gas temperature at 350 °C with a flow rate of 11 L/min; gas (nitrogen) flow of 5 L/min; capillary voltage of 2.0 kV; nozzle voltage of 500 V; gas temperature at 250 °C; nebulizer pressure of 60 psi. ACR was identified by multiple reaction monitoring (MRM) of the two channels. The precursor ion $[\text{M} + \text{H}]^+ 72$ was fragmented, and product ions 55 (collision energy of 9 V) and 44 (collision energy of 12 V) were monitored. Chromatographic separation was completed in 8 min, and ACR was eluted in 5.07 min. Quantification of ACR was based on a calibration curve built in the range between 1 and 100 $\mu\text{g}/\text{L}$. The LOD and LOQ values for acrylamide were 0.45 and 1.5 $\mu\text{g}/\text{kg}$ based on signal-to-noise ratios of 3 and 10, respectively.

Analysis of 5-Hydroxymethylfurfural. The obtained aqueous extract described above was subjected to Carrez clarification, and then it was filtered through a 0.45 μm syringe filter and collected into the autosampler vial. HMF analysis was performed as described by Hamzalıoğlu and Gökmen¹² by using Agilent 1200 HPLC system (Waldbronn, Germany) consisting of a diode array detector (DAD), a quaternary pump, a temperature-controlled oven, and an autosampler. The samples were analyzed using an Atlantis dC18 column (250 \times 4.6 mm i.d., 5 μm) at 25 °C. The mobile phase was an isocratic mixture of 10 mM formic acid solution and acetonitrile (90:10, v/v) at a flow rate of 1 mL/min. The wavelength was set to 285 nm. The quantification of HMF was performed by using a calibration curve built in the range between 1 and 10 $\mu\text{g}/\text{mL}$ (1, 2, 5, and 10 $\mu\text{g}/\text{mL}$). The LOD and LOQ values for HMF were 0.020 and 0.067 mg/kg based on signal-to-noise ratios of 3 and 10, respectively.

Analysis of 3-Deoxyglucosone. Previously prepared coextracts were precipitated with acetonitrile (1:1) and centrifuged at 15000 g for 5 min. α -Dicarbonyl compounds were derivatized by the procedure described by Kocadağlı and Gökmen.¹⁵ 150 μ L sodium phosphate buffer (pH 7) and 150 μ L 0.2% *o*-phenylenediamine solution containing 10 mM diethylenetriaminepentaacetic acid (DETAPAC) were added to 500 μ L of supernatant. The mixture was filtered through a 0.45 μ m filter, and the filtrate was collected into a vial prior to analysis. 3-DG was identified by Agilent Ultivo Triple Quadrupole MS coupled to Agilent 1260 HPLC in positive mode. Chromatographic separation was achieved with a Zorbax Eclipse XDB-C18 column (4.6 \times 150 mm, 5 μ m), and a gradient mixture of 1% formic acid in water (A) and 1% formic acid in methanol (B) were used as the mobile phase. The gradient mixture starting with 40% A was conditioned for 8 min and then increased to 80% A in 2 min and held for 3 min. The injection volume was 10 μ L. The electrospray source had the following settings: capillary voltage of 2.0 kV; nozzle voltage of 500 V; gas temperature of 250 $^{\circ}$ C; and sheath gas temperature of 400 $^{\circ}$ C with a flow rate of 12 L/min. Nebulizer pressure was set to 60 psi and the gas (N_2) flow rate was 10 L/min. Data were acquired in selected ion monitoring (SIM) mode. For the quantitation of 3-DG, the recorded SIM ion of the quinoxaline derivative of 3-DG was 235.2. Working solutions for calibration were prepared in acetonitrile:water (50:50, v/v) in the concentration range between 0.1 and 5 mg/kg. The LOD and LOQ values for 3-DG were 0.003 and 0.010 mg/kg based on signal-to-noise ratios of 3 and 10, respectively.

Multiresponse Kinetic Modeling. A comprehensive reaction mechanism was proposed comprising the formation pathways of ACR in the Maillard reaction during the roasting of nuts and seeds. Each step in the reaction network was characterized by reaction rate constants (k) as parameters. Differential equations were set for each elementary reaction step to introduce the reaction network to the mathematical model and solved by numerical integration. Determination of the reaction rate constants was estimated by nonlinear regression using the determinant criterion¹⁶ and numerical integration was performed by Athena Visual Studio software (AthenaVisual Inc.).

The concentrations of reactants and products were expressed as μ mol/kg of raw or roasted samples. Numerically solved equations were fitted to the experimental data, and the steps in the reaction network were evaluated by model discrimination. The goodness of fit of the models and also the highest posterior density (HPD) intervals of the estimated parameters were used to critique the kinetic models.

RESULTS AND DISCUSSION

Changes in Reactants, Intermediates, and Products.

The changes in the concentration of reactants (sucrose, free amino acids), intermediates (3-deoxyglucosone and 5-hydroxymethylfurfural), and ACR concentration were measured simultaneously during the roasting of nuts and seeds at different temperatures and times.

Sucrose was the main simple carbohydrate, whereas there were no detectable amounts of fructose and glucose due to the rapid degradation by the roasting process. Sucrose content in raw samples of sunflower seed, flaxseed, peanut, and almond was 3.2 ± 0.1 , 2.3 ± 0.1 , 4.0 ± 0.2 , and 3.4 ± 0.1 g/100 g, respectively. A gradual decrease in sucrose concentration was observed with roasting, depending on increasing temperature and time. In the harsh conditions (roasting at 200 $^{\circ}$ C for 20 min), the highest reduction in sucrose was seen in sunflower seeds (91%) compared with flaxseeds (68%), peanuts (57%), and almonds (53%).

Since asparagine is the direct precursor of ACR³, a change in the amount of free asparagine was recorded. The highest asparagine concentration was found in raw almond samples (1190.8 ± 151.0 mg/kg), followed by flaxseed (317.7 ± 7.4 mg/kg), peanut (273.7 ± 7.1 mg/kg), and sunflower seed

(264.6 ± 52.6 mg/kg), respectively. During the roasting process, the asparagine content showed a rapid decrease, and almost all asparagine was depleted at the end of the longest process time at all three temperatures.

The other free amino acids may affect ACR formation by participating in the Maillard reaction through their reaction with carbonyl compounds. Therefore, the levels of other free amino acids were also monitored. In raw samples total free amino concentration was 4051.5 ± 899.4 , 3064.7 ± 56.7 , 2453.6 ± 753.2 , and 4217.7 ± 493.1 mg/kg for sunflower, flaxseed, peanut, and almond, respectively. Total free amino acid content decreased by 77–89% in samples roasted at 160 $^{\circ}$ C for 60 min, 90–97% at 180 $^{\circ}$ C for 40 min, and 93–98% at 200 $^{\circ}$ C for 20 min.

In raw samples, there was a trace amount of 3-DG, whereas in raw sunflower seed, it was measured to be 5.5 mg/kg, and this may be attributed to improper storage conditions. The formation of 3-DG was induced by roasting in all samples. The level of 3-DG in sunflower and flaxseed samples increased to a certain extent at 180 and 200 $^{\circ}$ C and then followed a decreasing trend during prolonged roasting times. In other samples, 3-DG showed a continuously increasing trend with an increasing roasting time. The highest 3-DG concentration was detected in sunflower seed roasted at 160 $^{\circ}$ C for 60 min (17.8 ± 0.9 mg/kg), while the concentration of 3-DG in the other nuts and seeds reached 12 mg/kg. The increase in the concentration of dicarbonyl compounds in the early stages of roasting can be explained by their formation through sugar degradation or Maillard reaction, whereas their degradation reactions and their contribution in advanced stages of Maillard reaction by further reactions with side chains of peptides or proteins might be an explanation for the decrease in their concentration.

The concentration of HMF in all samples rapidly increased, following a lag phase. This lag phase lasted longer, especially at low roasting temperatures. The highest levels of HMF were observed in sunflower seeds roasted at 180 $^{\circ}$ C for 30 min (247.0 ± 8.3 mg/kg) followed by almond (166.2 ± 21.1 mg/kg), flaxseed (155.4 ± 4.0 mg/kg), and peanut (144.4 ± 16.7 mg/kg). In sunflower seed, flaxseed, and peanut samples roasted at 200 $^{\circ}$ C, HMF could not reach levels as high as those in the samples roasted at 180 $^{\circ}$ C, and moreover, HMF in sunflower and flaxseed began to degrade at 200 $^{\circ}$ C within 15 min. However, in almond samples, a continuous sharp increase was observed in the concentration of HMF with increasing temperature and time.

ACR followed a similar trend in all of the roasted samples. The levels of ACR rapidly increased to a certain extent and started to decrease afterward due to the prolonged roasting times. The amount of detected ACR is the net difference between the amount of ACR generated and eliminated simultaneously during the roasting process, and these reactions cannot be distinguished from each other. Therefore, the decrease in the ACR concentration could be explained by the depletion of the reactants or the elimination of ACR becoming more predominant.⁴ Since the starting point of this decrease varies according to the reaction medium and roasting temperature, the same pattern was not observed in all samples. Higher temperatures or longer roasting times at a certain temperature might be needed for acrylamide degradation to dominate over acrylamide formation. However, the difference in patterns does not indicate that the formation mechanism is different. The highest ACR content among all the samples was

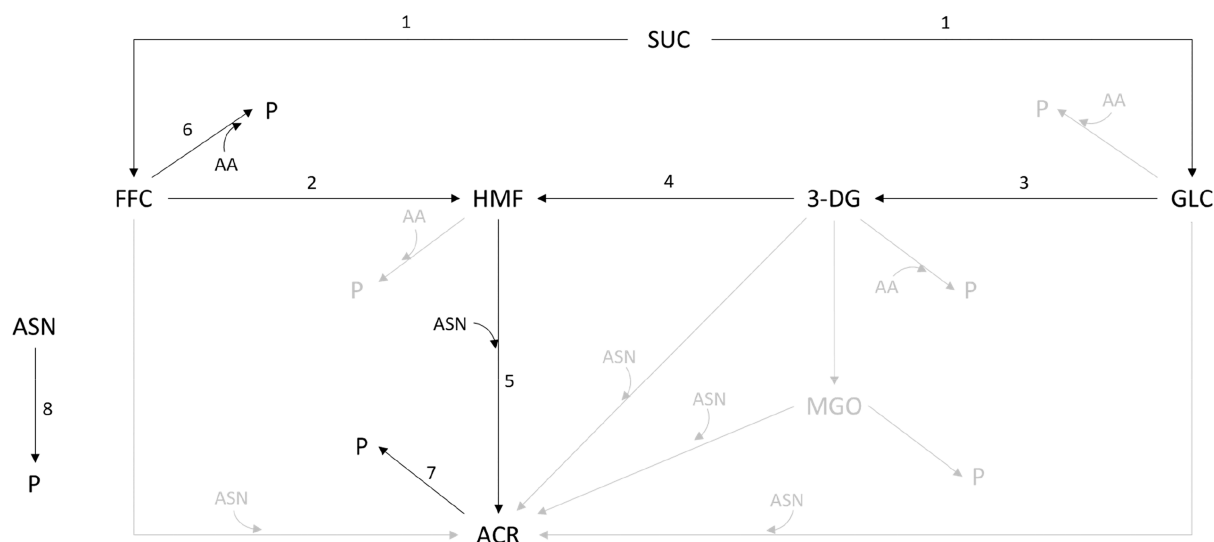


Figure 1. Comprehensive model for acrylamide formation in nuts and seeds during roasting. The gray steps are not included in the proposed kinetic model. SUC: Sucrose; GLC: Glucose; FFC: Fructofuranosyl cation; AA: Total amino acids; ASN: Asparagine; 3-DG: 3-Deoxyglucosone; MGO: Methylglyoxal; HMF: 5-Hydroxymethyl furfural; ACR: Acrylamide; P: Products.

found in almonds ($3127.0 \pm 130.8 \mu\text{g}/\text{kg}$) after roasting at 200°C for 15 min due to the higher amount of free asparagine compared to the other samples. Almond was followed by flaxseed ($1036.7 \pm 29.4 \mu\text{g}/\text{kg}$), sunflower ($981.7 \pm 196.6 \mu\text{g}/\text{kg}$), and peanut ($378.0 \pm 64.5 \mu\text{g}/\text{kg}$) with an ACR content of almost one-tenth of almonds. It was also found that the ACR content in flaxseed, sunflower, and especially almond was significantly higher when compared to many ACR-rich foods such as French fries or potato crisps ($300\text{--}2300 \mu\text{g}/\text{kg}$).

Hamzalıoğlu and Gökmen¹² also observed an increase followed by a decrease in the concentration of α -dicarbonyl compounds and reported the highest concentration of 3-DG in coffee as $1418.88 \pm 3.70 \text{ mg}/\text{kg}$ at the end of 10 min of roasting at 200°C . In a study carried out by Berk et al.,¹¹ the highest 3-DG concentration in sesame seeds was found to be $6.9 \pm 0.4 \text{ mg}/\text{kg}$ after 30 min of roasting at 180°C and $5.7 \pm 0.9 \text{ mg}/\text{kg}$ at 220°C for 10 min of roasting, respectively. Cämmerer and Kroh¹⁷ stated that the deoxyhexosuloses detected in peanuts increased with roasting, and this increase was obviously due to the increase in the reaction temperature, not the reaction time. In a previous study on hazelnut roasting, the highest amount of 3-DG was found as $6.7 \pm 0.1 \text{ mg}/\text{kg}$ dw at the end of roasting at 150°C for 120 min.¹⁸ Batool et al.¹⁹ investigated α -dicarbonyl compounds in commercially available edible seeds. In hazelnut samples, they reported the maximum 3-DG content as $3.80 \pm 0.28 \text{ mg}/\text{kg}$, whereas it was $2.89 \pm 0.22 \text{ mg}/\text{kg}$ in peanut samples.

In a study carried out by Agila and Barringer²⁰ in which the level of HMF in sweet almonds was investigated, it was stated that the amount of HMF increased depending on the increase in temperature, and the highest amount of HMF ($905 \mu\text{g}/\text{L}$) was reached after 20 min of heat treatment at 177°C . In another study, the amounts of HMF formed by roasting hazelnuts at 150°C for 60 min and 175°C for 30 min were determined as $8.0 \pm 0.0 \text{ mg}/\text{kg}$ and $66.5 \pm 5.6 \text{ mg}/\text{kg}$, respectively.²¹ Göncüoğlu Taş and Gökmen¹⁸ roasted hazelnut samples at different times and temperatures and stated HMF amount reached up to $278 \pm 0.7 \text{ mg}/\text{kg}$ dw within 120 min of roasting at 170°C . Batool et al.¹⁹ reported the highest HMF concentration in commercially available hazelnuts and peanuts

as 48.05 ± 2.18 and $75.44 \pm 3.13 \text{ mg}/\text{kg}$, respectively. Considering the daily consumption amounts of nuts (30 g), the highest HMF intake is from sunflower ($7.4 \text{ mg}/\text{day}$). Although the safe consumption amount of HMF is not clear, it is estimated that people ingest up to 150 mg of HMF per day through various foods.²² However, it should be considered that HMF is not only taken from these foods.

Schlormann et al.²³ reported that the ACR content of almonds and pistachios was found to be 1220 and $88 \mu\text{g}/\text{kg}$ after the roasting process at 170.8°C for 15 min and 185.1°C for 21 min, respectively. In another study, while ACR could not be detected in raw almond samples, it was determined that the amount of ACR increased with roasting at temperatures ranging from 129 to 182°C , and reached $907 \mu\text{g}/\text{kg}$ at 182°C within 5.7 min.²⁴ In a study by Amrein et al.,²⁵ the highest amount of ACR in commercially roasted almonds was determined as $2147 \mu\text{g}/\text{kg}$. Amrein et al.²⁶ also compared the formation of ACR in different almond cultivars and found the highest ACR content ($1681 \mu\text{g}/\text{kg}$) after 12.5 min of heat treatment at 162°C in the cultivar of Carmel, which also has the highest asparagine content ($2760 \text{ mg}/\text{kg}$). In a study conducted by Nematollahi et al.,²⁷ the concentration of ACR increased up to 152.55 ± 13.59 and $171.75 \pm 15.31 \mu\text{g}/\text{kg}$ among 6 types of roasted peanut and 3 types of roasted sunflower samples, respectively. The ACR content of roasted sunflower seed was found to be $66 \mu\text{g}/\text{kg}$ in another study.²⁸ Ölmez et al.²⁹ and De Paola et al.³⁰ reported the highest ACR content in roasted peanuts as 66 and $42.9 \mu\text{g}/\text{kg}$, respectively.

Kinetic Modeling. The current challenge in this study was to propose a kinetic model for ACR formation in low moisture, sucrose-rich but reducing-sugar-poor food systems such as nuts and seeds. Since the water content of the reaction medium affects the course of chemical reactions, it is an inaccurate approach to interpret dry systems with kinetic models proposed for aqueous systems. For this purpose, a comprehensive model including all reported pathways in ACR formation occurring in low moisture conditions was built and presented in Figure 1. As the aim of this study was to reveal a simple kinetic model for ACR formation, the comprehensive model was simplified by considering the

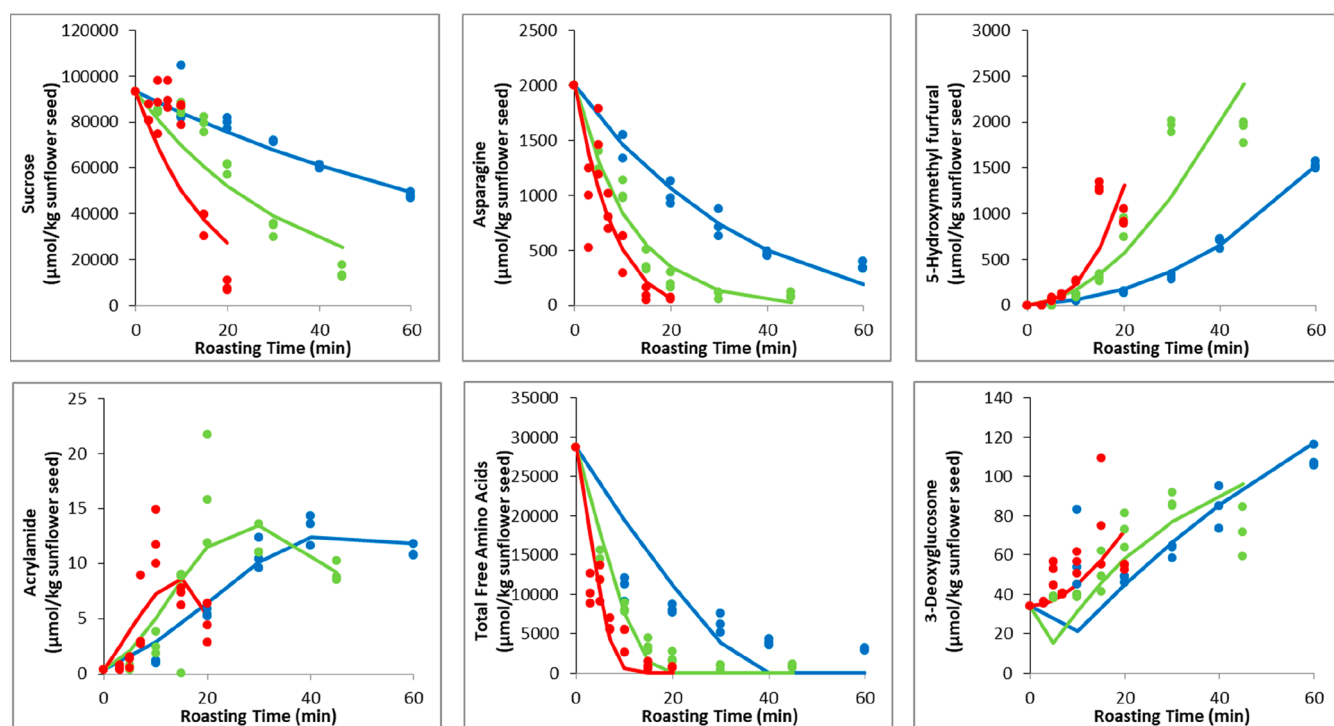


Figure 2. Kinetic model fits (lines) to the obtained experimental data (symbols) of reactants and products during roasting of sunflower seed. Blue color for markers and lines designates 160 °C, green 180 °C, and red 200 °C.

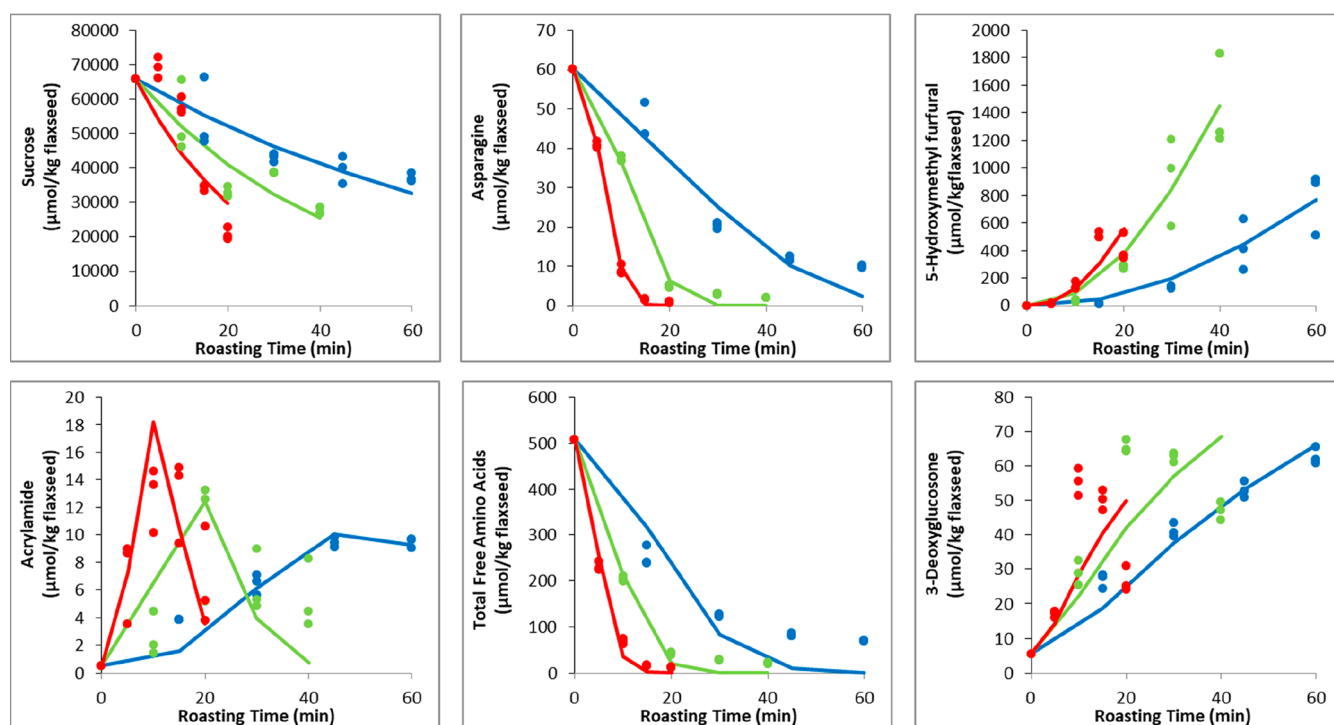


Figure 3. Kinetic model fits (lines) to the obtained experimental data (symbols) of reactants and products during roasting of flaxseed. Blue color for markers and lines designates 160 °C, green 180 °C, and red 200 °C.

important and dominant reaction pathways identified in previous studies. The reaction network was translated into a mathematical model to fit the experimental data to the proposed model. Hence, differential equations given in Appendix A were written for each reaction step and solved by numerical integration.³¹ The kinetic model fits of the

comprehensive model are represented in Figures S1–4. Further simplifications were done to increase the precision of the estimated parameters by excluding kinetically insignificant pathways one by one, which were illustrated in gray. In this context, the importance of steps was tested by including or omitting certain steps from the reaction network. The

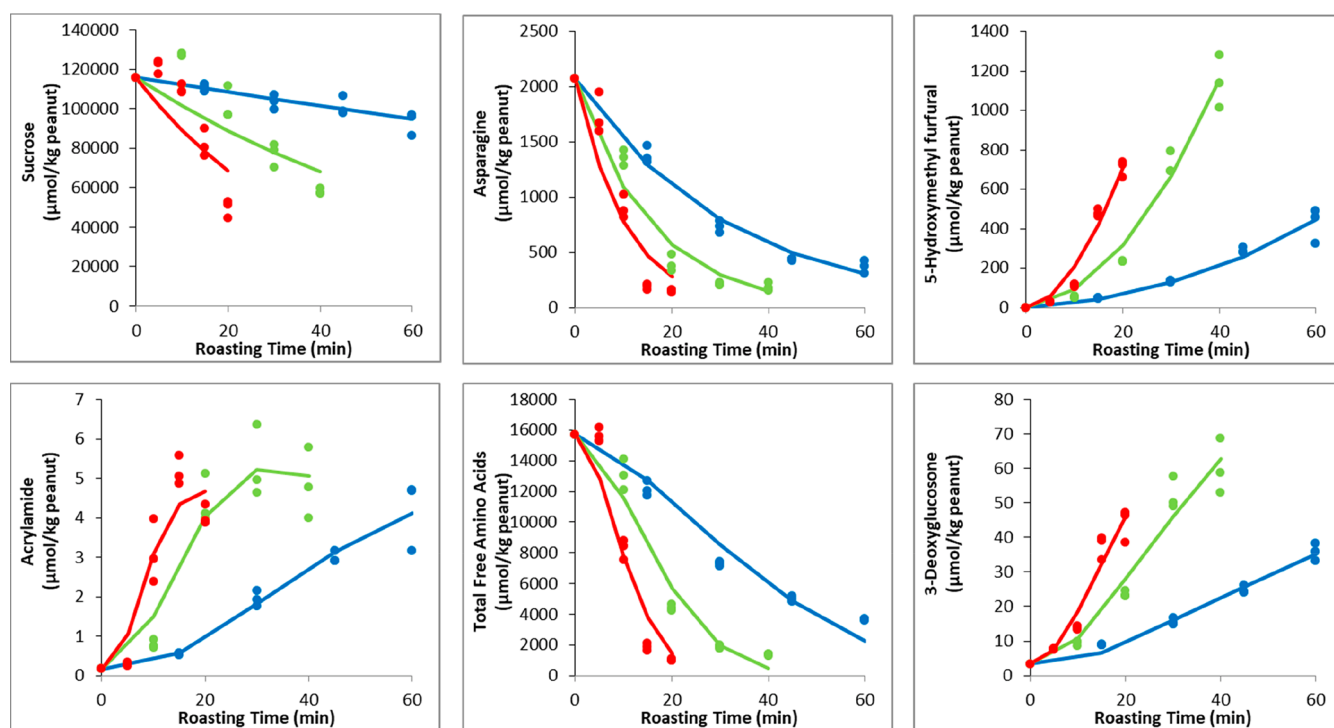


Figure 4. Kinetic model fits (lines) to the obtained experimental data (symbols) of reactants and products during roasting of peanut. Blue color for markers and lines designates 160 °C, green 180 °C, and red 200 °C.

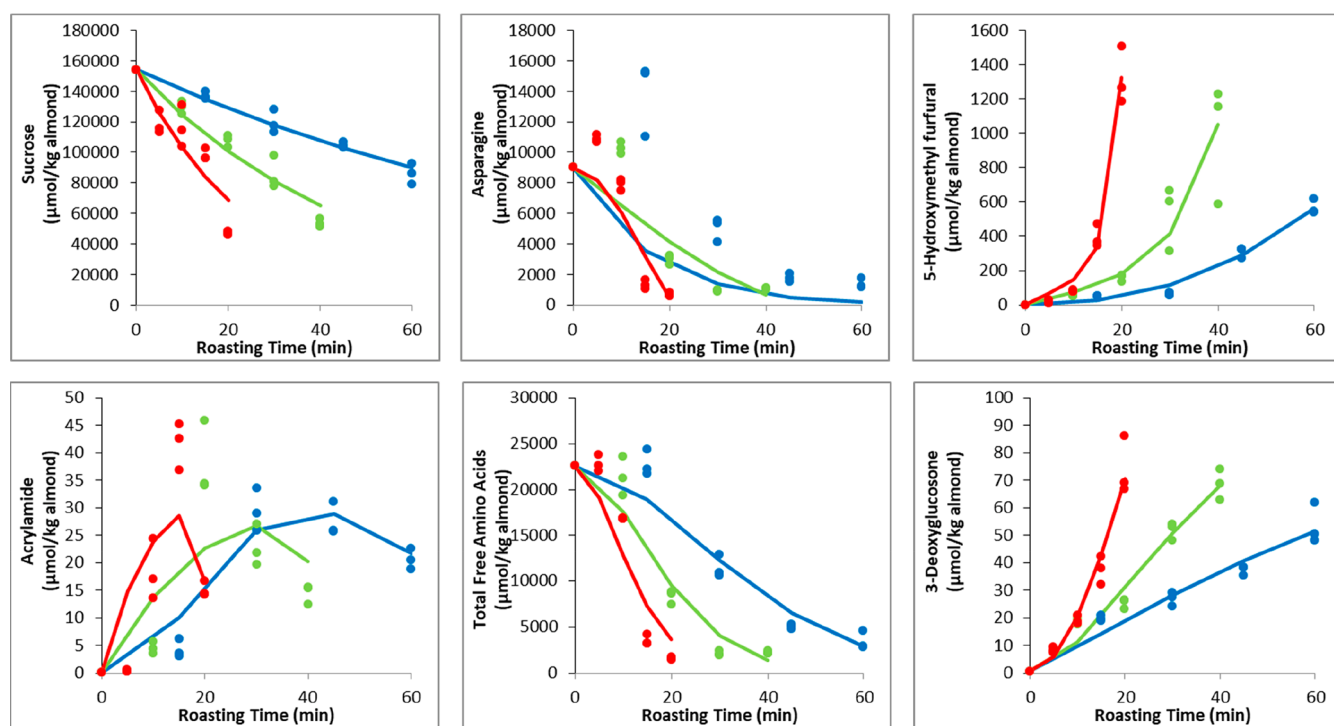


Figure 5. Kinetic model fits (lines) to the obtained experimental data (symbols) of reactants and products during roasting of almond. Blue color for markers and lines designates 160 °C, green 180 °C, and red 200 °C.

mathematical models were built by setting up the corresponding differential equations and compared with the observed data. By doing this, it was possible to reveal whether some of the steps are a fast step and can be excluded from the kinetic model, or whether it is an important step under the specified conditions. Excluding the steps mentioned as kinetically

insignificant from the model, did not cause a bad estimation, but also when they were included in the model, the reaction rates of these steps were found to be insignificant, and including these steps caused an increase in the number of unknown parameters. Exceptions for each step were discussed hereinafter in detail. In addition, many of the reactions were

Table 1. Estimated Reaction Rate Constants (k , $\text{min}^{-1} \times 10^3$) with 95% Highest Posterior Density (HPD) Intervals at Different Temperatures According to the Proposed Model for Acrylamide Formation during Roasting of Samples

elementary reaction step	sunflower seed			flaxseed			peanut			almond		
	160 °C	180 °C	200 °C	160 °C	180 °C	200 °C	160 °C	180 °C	200 °C	160 °C	180 °C	200 °C
1. SUC → FFC+GLC	10.6 ±1.38	29.2 ±6.03	61.9 ±19.89	11.78 ±1.8	23.7 ±4.06	39.9 ±12.4	3.4 ±0.47	13.3 ±3.56	26.2 ±8.69	9.0 ±0.64	21.4 ±2.2	40.4 ±7.49
2. FFC → HMF	0.7 ±0.68	0.0 ±0.0	4.7 ±3.19	0.0 ±0.0	0.0 ±0.0	0.0 ±0.0	1.3 ±0.66	1.6 ±0.58	1.9 ±0.78	0.0 ±0.0	3.0 ±1.96	14.1 ±2.82
3. GLC → 3-DG	1.2 ±0.25	1.4 ±0.28	0.1 ±0.02	0.8 ±0.14	1.7 ±0.30	1.6 ±0.48	0.3 ±0.16	0.2 ±0.14	0.2 ±0.17	0.4 ±0.31	0.1 ±0.05	0.1 ±0.01
4. 3-DG → HMF	419.4 ±75.03	939.2 ±178.7	0.0 0±0.0	370.2 ±52.55	951.2 ±189.2	1100.1 ±342.1	142.6 ±94.06	118.7 ±109.2	153.6 ±184.4	450.2 ±381.9	108.4 ±75.6	0.0 ±0.0
5. HMF + Asn → ACR	16.5 ±7.0	8.8 ±4.48	135.9 ±180.2	126.3 ±32.51	677.9 ±236.2	3514.2 ±1102	1.6 ±0.78	5.4 ±2.99	12.7 ±11.6	28.1 ±25.81	138.5 ±126	572.0 ±184.4
6. FFC+AA → P1	1022.1 ±30710	85.2 ±129.7	57.9 ±63.29	5.9 ±1.94	12.3 ±2.38	23.6 ±7.32	8.4 ±3.57	5.3 ±2.14	6.6 ±3.14	1.4 ±0.33	1.9 ±0.5	2.6 ±0.95
7. ACR → P2	424.6 ±187.30	110.2 ±71.97	2091.7 ±2151	44.9 ±15.15	172.2 ±60.13	219. ±50.73	41.4 ±35.1	193.7 ±144.7	544.4 ±638.1	132.5 ±535.4	4605.6 ±3659	21412.5 ±5286
8. Asn → P3	30.8 ±3.29	86.3 ±9.14	126.2 ±34.36	20.8 ±4.86	27.1 ±10.39	38.5 ±9.49	31.6 ±2.01	63.9 ±9.24	97.1 ±24.49	65.0 ±82.67	27.9 ±21.34	0.0 ±0.0

shown as unimolecular and single step. There are many more reactions shown like this and not shown in this model but that take place under the Maillard reaction. These can be both multistep and bimolecular reactions. However, all these were not shown in the model, since the including of all these in a model that shows the mechanism of acrylamide formation would be meaningless in terms of the difference in concentrations and would increase the number of unknown parameters. Finally, a simple and adequate kinetic model for ACR formation was finally proposed by using six responses. The proposed reaction network was composed of degradation of sucrose to glucose and fructofuranosyl cation (FFC), 3-DG formation, HMF formation through 3-DG or FFC, ACR formation through the reaction of asparagine with HMF, and elimination reactions of FFC, ACR, and free asparagine. The fits of the proposed kinetic model are represented in Figures 2–5. The markers indicate the obtained experimental data at 160, 180, and 200 °C for each roasted sample whereas the lines show the estimated kinetic model fits. The estimated reaction rate constants are given in Table 1. As mentioned before, the reactions included in the model can consist of several steps. Since these intermediate reactions occur very quickly and consecutively it is difficult to follow the intermediates; they were shown as a single step in the simplified kinetic model. Moreover, the composition and structural differences of the studied nuts and seeds, the complexity of the reaction studied, the roasting temperature, and the extremely low amounts of some of the reaction products measured can affect the calculated rate constants. Therefore, the rate constants of the different reaction steps in Table 1 were used to compare with each other to determine the predominant pathways. It is concluded that lower rate constants calculated for certain elementary reaction steps indicate that the complex reaction proceeds predominantly from another reaction step. The validity of the kinetic model was decided according to the goodness of fit values, and the reaction rate constants were calculated by a numerical solution of the differential equations that explain the model by Athena Visual Studio Software. The accuracy of the calculated rate constants was shown in Table S2.

Degradation of Sucrose. Although sucrose is not a reducing sugar, it indirectly participates in the formation of ACR by forming new carbonyl sources for the Maillard reaction by thermal degradation. In low-moisture systems, sucrose degrades to glucose and FFC through cleavage of the glycosidic bond, and this step is considered the main mechanism for the degradation of sucrose. The formation of FFC from fructose was not included in the comprehensive model since it was reported that this step is difficult to occur.³¹ In addition, the interconversion of glucose and fructose through 1,2-enolization¹⁰ was also excluded from the model in order to decrease the number of parameters and thus increase the precision of the estimation process. The best model fit was obtained, and the concentrations of sucrose were well estimated when only degradation of sucrose to glucose and FFC was included in the model. The increase in the roasting temperature caused a substantial increase in the reaction rate constants of sucrose degradation (k_1) in all roasted samples with relatively higher values in sunflower seeds (Table 1).

Formation of α -Dicarbonyl Compounds. The α -dicarbonyl compounds that have been reported to be involved in ACR formation such as 3-DG and methylglyoxal (MGO) were included in the comprehensive model. FFC can react with an amine to form a fructofuranosyl amine, which is rearranged to form a Heyns product (HP). The reaction of glucose with an amine compound followed by the rearrangement to a more stable compound, AP, is also possible. In later stages, the degradation of AP and HP leads to the formation of 3-DG. However, in previous studies, the reaction rate constants of the 3-DG formation step through AP or HP were found to be very low or zero which means they were kinetically less important in these circumstances.^{11,12,18} Hence, side reaction steps such as these were not indicated, even in the comprehensive model. Apart from these, 3-DG can also be formed through the removal of one molecule of water from glucose in caramelization.³² In this context, the model fits were well estimated in the case of adding only this route (k_3) for the formation of 3-DG. It was determined that the rate constant of this reaction step (k_3) was lower in the samples roasted at 200 °C compared to those at other roasting temperatures.

Additionally, it should be considered that there were deviations in the 3-DG model fits of flaxseed and sunflower seed samples at 180 and 200 °C only in prolonged roasting times.

The predominant short-chain α -dicarbonyl MGO was also included in the comprehensive model as it was stated by Stadler et al.³⁴ that MGO may also take part in the formation of ACR. It was reported that one of the possible formation pathways of MGO is from 3-DG via retro-aldolization.³⁵ However, previous studies reported that more important steps were determined in ACR formation, and the MGO pathway was less significant in ACR formation compared to other α -dicarbonyl pathways.³⁴ Besides, MGO formation and elimination steps were included in the comprehensive model, but the model could not fit well with observed data (data not shown). Therefore, these steps were omitted from the model, and a better model fit was obtained.

Formation of HMF. There are generally two formation pathways considered for the formation of HMF: dehydration of FFC (k_2) and 3-DG (k_4).³⁶ The cyclic form of FFC facilitates its conversion to HMF under dry conditions.³² HMF is also generated by the removal of 3 molecules of water from glucose through 3-DG.³³

It was determined that the 3-DG pathway was predominant in HMF formation at 160 and 180 °C. At 200 °C, the FFC pathway (k_2) became dominant in almonds and sunflower seeds, whereas in others, HMF was still formed mainly through 3-DG (k_4). The reason for the 3-DG pathway becoming quantitatively less significant in the formation of HMF in almond samples roasted at 200 °C might be attributed to a decrease in the rate of 3-DG formation from glucose (GLC). In addition, the conversion of FFC to other products (k_6) was found to be kinetically more important than the dehydration of FFC to HMF (k_2) in all samples, except almonds.

However, FFC is known to be an important precursor for HMF, and it should be considered that the lower rate constants of the FFC pathway (k_2) did not mean that this step is unimportant. FFC plays an important role in explaining the amount of HMF formed. The higher rate constants of the 3-DG pathway (k_4) might also be associated with the fact that FFC could not be measured experimentally, and this multistep conversion was shown as a single step in the model. These observations were also supported by the findings of Göncüoğlu Taş and Gökmen¹⁸ who reported that the calculated reaction rate constants of HMF formation via FFC were relatively lower than the rate constants of HMF formation via 3-DG. However, they also stated that the model prediction obtained when the FFC pathway was excluded in the same kinetic model was not compatible with the experimental data, and therefore the increase in the amount of HMF could not be explained by only the 3-DG pathway. By doing so, they also indicated that the HMF formation step from FFC is crucial, although the rate constant was found to be lower.

Formation of ACR. Asparagine provides the backbone of ACR, and the formation of ACR from asparagine can occur through the involvement of various carbonyl compounds. Parker et al.³⁷ defined two pathways for the formation of ACR as the specific and generic amino acid pathways. The reaction of asparagine directly with reducing sugar to form ACR was called a specific amino acid route, whereas the generic amino acid route is the reaction of asparagine with dicarbonyls/hydroxycarbonyls formed through AP of reducing sugars and α -amino acids. They also drew attention to the importance of the contribution of both pathways in ACR formation.

According to them, the predominance of the reaction pathways is affected by the composition of the medium and the process parameters. Especially, more reactive amino acids than asparagine can be the source of precursors required for the generic amino acid pathway. In addition to these reaction pathways, the formation of ACR as a result of the reaction of FFC with asparagine was also included in the comprehensive model, since it was reported by Perez Locas and Yaylayan³² that FFC can react with amines.

Another source of ACR formation was found to be HMF. The role of HMF in the ACR formation mechanism was first described by Gökmen et al.³⁸ In this study, the asparagine-HMF model system produced relatively higher amounts of acrylamide than the asparagine-GLC model system under the same reaction conditions at temperatures exceeding 120 °C, and obtained kinetic data showed that HMF was more effective than glucose in the formation of ACR from asparagine in low-moisture systems. This was explained by the fact that HMF has a lower melting point and is therefore more thermodynamically favorable to forming amine condensation products. HMF also contributes to the formation of ACR in the presence of asparagine by taking part in the Maillard reaction during heat treatment due to its carbonyl function. Since HMF is involved in the formation of ACR in this way, FFC also contributes to the formation of ACR in another way by dehydrating to HMF, as well as reacting with asparagine to form ACR as a carbonyl source.

When the involvement of different carbonyl compounds in ACR formation was compared in light of the results obtained in previous studies,³⁹ it was concluded that the most predominant pathway in dry systems was ACR formation in the presence of HMF.^{11,12,40} Indeed, in previous studies and for the comprehensive model mentioned in this study, the reaction rate constants for ACR formation pathways from carbonyl sources other than HMF were calculated as zero or relatively low. In a study by Stadler et al.,³⁴ the reaction between asparagine and glucose was found kinetically more important than the reaction of asparagine with α -dicarbonyl compounds in ACR formation. Additionally, Nguyen et al.,⁴⁰ in a study investigating the effect of sugar type on ACR formation in biscuits, determined that the effect of glucose was negligible when compared to fructose. Similar results to model systems were also obtained in the food matrix. Hamzalıoğlu and Gökmen¹² calculated the reaction rate constants of ACR formation from FFC and glucose as zero during the roasting process of coffee. In another study, Berk et al.¹¹ found that the reaction of asparagine with HMF was more important than with glucose. To sum up, since the aim was to determine a simple model, only the involvement of HMF (k_5) was included, and the other carbonyl sources were excluded in the proposed model for the conversion of asparagine to ACR. In the proposed kinetic model considered in this way, it was observed that the model was well-fitted to the experimental data. It can be concluded that the pathway comprising HMF is kinetically important in the formation of ACR through Maillard reaction during the roasting process in dry systems with low reducing sugar content but with a significant amount of sucrose.

When the rate constants of ACR formation were examined, it was seen that the estimated parameters increased with increasing temperature. However, the highest rate constant was determined in the flaxseed samples as a result of roasting at 200 °C. ACR can also undergo further reactions with amino

acids which are called Michael-type additions.⁴¹ However, unimolecular degradation without the involvement of amino acids fitted better to experimental data instead of the bimolecular reaction of ACR for the elimination of degradation into products (k_7). According to the results, the reaction rate constant of this step increased with temperature in the samples as in the case of the formation reaction except for sunflower, while the highest rate constant was observed in almonds. Additionally, except in a flaxseed sample, this elimination step was found to be more important than the formation rate of ACR (Table 1). Knol et al.⁴² also proposed a kinetic model that suggests ACR is an intermediate not an end-product of the Maillard reaction and undergoes further degradation reactions.

During the roasting of oil-rich nuts and seeds, lipid oxidation also occurs simultaneously with sucrose degradation reactions. As the lipid peroxidation products carry a carbonyl moiety, they act as precursors and trigger the formation of acrylamide. However, it is difficult to distinguish the origin of dicarbonyl compounds due to the complex nature of foods as dicarbonyl compounds can also be formed by sucrose degradation. In addition, the aim of this study was not to investigate the effects of lipid peroxidation products on acrylamide formation but to reveal which pathway is more predominant. Therefore, the effect of the lipid peroxidation products was ignored in the proposed model. The fact that lipid oxidation was ignored in the proposed model does not mean that such a contribution does not exist. It was stated in our previous studies that the presence of lipids in the reaction medium contributes to the formation of acrylamide.⁴³ However, it was determined that secondary lipid peroxidation products, which may contribute to acrylamide formation, started to increase after 5 min during roasting of coffee at 220 °C. In this study, such high temperatures were not reached during roasting, and even the applied 200 °C was an extreme condition when compared to industrial parameters. In addition, the kinetic model was evaluated with a goodness of fit. Although acrylamide showed a good fit with experimental data, in cases where the acrylamide data did not fit well, it could be attributed to the effect of dicarbonyl compounds formed from lipid oxidation on acrylamide formation was significant.

It has been shown in different studies that asparagine can also degrade to products such as aspartic acid and fumaric acid during roasting.⁴⁴ The decomposition of asparagine to several products was also indicated in the model (k_8) to obtain the best model fit, and k_8 increased with increasing temperature in all samples except almond.

This kinetic model was proposed for temperatures at which nuts and seeds are roasted or baking temperatures of products to which they are added as ingredient. In addition, the reaction routes may change, and different compounds may be formed, especially at extreme temperatures. As a result, the model might not show a good fit at different temperatures, and the fit might deviate with the change in temperature. However, this does not mean that the steps indicated as dominant are not important.

In conclusion, a simplified kinetic model was suggested for the formation of ACR during roasting in low-moisture systems by this study. The rate constants for elementary reaction steps were estimated by multiresponse kinetic modeling of sucrose, total free amino acids, asparagine, HMF, 3-DG, and ACR concentrations in sunflower seed, flaxseed, peanut, and almond roasted at 160, 180, and 200 °C. Although the proposed model does not exactly express the whole Maillard reaction

mechanism, it explains the measured responses related to the formation of ACR. The proposed model consisted of reaction steps including sucrose degradation, formation of α -dicarbonyl compounds, HMF, and ACR. The conversion of free asparagine, FFC, and ACR to different products was also included in the proposed model, whereas the further conversions of glucose, 3-DG, and HMF were excluded. The contribution of HMF to the formation of the ACR was also demonstrated. Due to its low melting temperature, HMF is a thermodynamically more favorable reactant in the formation of ACR during the roasting of low-moisture food systems.

Since we aimed to obtain a simple and inclusive model in this study, we first proposed a reaction scheme by eliminating the pathways that were determined not to be kinetically important for the formation of ACR in our previous studies. Undoubtedly, care was taken not to cause worse posterior probability while neglecting these steps. Here, we determined that these previously proposed models are robust for low-moisture sucrose-rich foods, as in the example of nuts and seeds. By this study, without considering botanical nomenclature, it became possible to predict changes quantitatively in any temperature–time combination in other foods with a composition similar to that of the studied foods. Therefore, this model allows us to strike a balance between the benefits and collateral damage of heat treatment by optimizing process conditions. In addition, it was determined that this proposed model can create a basis for mitigation strategies of ACR formation, and further studies on different nuts and seeds also should be performed to improve the accuracy of the model.

■ APPENDIX A

Differential equations, which are built from the kinetic model of nuts and seeds given in Figure 1.

$$\frac{d[\text{SUC}]}{dt} = -k_1[\text{SUC}] \quad (1)$$

$$\frac{d[\text{Asn}]}{dt} = -k_5[\text{HMF}][\text{Asn}] - k_8[\text{Asn}] \quad (2)$$

$$\frac{d[\text{HMF}]}{dt} = k_2[\text{FFC}] + k_4[3 - \text{DG}] - k_5[\text{HMF}][\text{Asn}] \quad (3)$$

$$\frac{d[\text{ACR}]}{dt} = k_5[\text{HMF}][\text{Asn}] - k_7[\text{ACR}] \quad (4)$$

$$\frac{d[\text{AA}]}{dt} = -k_6[\text{FFC}][\text{AA}] \quad (5)$$

$$\frac{d[3 - \text{DG}]}{dt} = k_3[\text{GLC}] - k_4[3 - \text{DG}] \quad (6)$$

$$\frac{d[\text{GLC}]}{dt} = k_1[\text{SUC}] - k_3[\text{GLC}] \quad (7)$$

$$\frac{d[\text{FFC}]}{dt} = k_1[\text{SUC}] - k_2[\text{FFC}] - k_6[\text{FFC}][\text{AA}] \quad (8)$$

$$\frac{d[P_1]}{dt} = k_6[\text{FFC}][\text{AA}] \quad (9)$$

$$\frac{d[P_2]}{dt} = k_7[\text{ACR}] \quad (10)$$

$$\frac{d[P_3]}{dt} = k_g[\text{Asn}] \quad (11)$$

■ ASSOCIATED CONTENT

SI Supporting Information

The Supporting Information is available free of charge at <https://pubs.acs.org/doi/10.1021/acsfoodscitech.3c00359>.

MRM transitions used to detect individual free amino acids; the accuracy of the calculated rate constants for the proposed simplified kinetic model; the kinetic model fits of the comprehensive model (PDF)

■ AUTHOR INFORMATION

Corresponding Author

Vural Gökmen – Food Quality and Safety (FoQuS) Research Group, Department of Food Engineering, Hacettepe University, 06800 Beytepe, Ankara, Turkey; orcid.org/0000-0002-9601-5391; Phone: 90-312-297-7108; Email: vgokmen@hacettepe.edu.tr; Fax: 90-312-299-2123

Author

Dilara Şen – Food Quality and Safety (FoQuS) Research Group, Department of Food Engineering, Hacettepe University, 06800 Beytepe, Ankara, Turkey; orcid.org/0000-0002-0238-703X

Complete contact information is available at: <https://pubs.acs.org/doi/10.1021/acsfoodscitech.3c00359>

Funding

This research did not receive any specific grant from funding agencies in the public, commercial, or not-for-profit sectors.

Notes

The authors declare no competing financial interest.

■ REFERENCES

- (1) Kalogeropoulos, N.; Chiou, A.; Ioannou, M. S.; Karathanos, V. T. Nutritional evaluation and health promoting activities of nuts and seeds cultivated in Greece. *Int. J. Food Sci. Nutr.* **2013**, *64* (6), 757–767.
- (2) WHO, I. A. R. C. *IARC monographs program on the evaluation of carcinogenic risks to humans – Some industrial-chemicals, Lyon, 15–22 February 1994 – Preamble. In Iarc Monographs on the Evaluation of Carcinogenic Risks to Humans – Vol 60: Some Industrial Chemicals* (pp. 13–33); Int Agency Research Cancer; Lyon, 1994.
- (3) Yaylayan, V. A.; Wnorowski, A.; Perez-Locas, C. Why asparagine needs carbohydrates to generate acrylamide. *J. Agric. Food Chem.* **2003**, *51*, 1753–1757.
- (4) De Vleeschouwer, K.; Van der Plancken, I.; Van Loey, A.; Hendrickx, M. E. Modelling acrylamide changes in foods: from single-response empirical to multiresponse mechanistic approaches. *Trends in Food Science & Technology* **2009**, *20* (3–4), 155–167.
- (5) Kroh, L. W. Caramelisation in food and beverages. *Food Chem.* **1994**, *51* (4), 373–379.
- (6) Capuano, E.; Fogliano, V. Acrylamide and 5-hydroxymethylfurfural (HMF): A review on metabolism, toxicity, occurrence in food and mitigation strategies. *LWT - Food Science and Technology* **2011**, *44* (4), 793–810.
- (7) Kocadağlı, T.; Gökmen, V. Multiresponse kinetic modelling of Maillard reaction and caramelisation in a heated glucose/wheat flour system. *Food Chem.* **2016**, *211*, 892–902.
- (8) Robert, F.; Vuataz, G.; Pollien, P.; Saucy, F.; Alonso, M.-I.; Bauwens, I.; Blank, I. Acrylamide Formation from Asparagine under Low-Moisture Maillard Reaction Conditions. 1. Physical and Chemical Aspects in Crystalline Model Systems. *J. Agric. Food Chem.* **2004**, *52* (22), 6837–6842.
- (9) Martins, S. I. F. S.; Jongen, W. M. F.; van Boekel, M. A. J. S. A review of Maillard reaction in food and implications to kinetic modelling. *Trends in Food Science & Technology* **2000**, *11* (9), 364–373.
- (10) Martins, S. I. F. S.; Van Boekel, M. A. J. S. A kinetic model for the glucose/glycine Maillard reaction pathways. *Food Chem.* **2005**, *90* (1–2), 257–269.
- (11) Berk, E.; Hamzalıoğlu, A.; Gökmen, V. Multiresponse kinetic modelling of 5-hydroxymethylfurfural and acrylamide formation in sesame (*Sesamum indicum* L.) seeds during roasting. *European Food Research and Technology* **2020**, *246* (12), 2399–2410.
- (12) Hamzalıoğlu, A.; Gökmen, V. 5-Hydroxymethylfurfural accumulation plays a critical role on acrylamide formation in coffee during roasting as confirmed by multiresponse kinetic modelling. *Food Chem.* **2020**, *318*, 126467.
- (13) Şen, D.; Gökmen, V. Kinetic modeling of Maillard and caramelization reactions in sucrose-rich and low moisture foods applied for roasted nuts and seeds. *Food Chem.* **2022**, *395*, 133583.
- (14) Gökmen, V.; Morales, F. J.; Ataç, B.; Serpen, A.; Arribas-Lorenzo, G. Multiple-stage extraction strategy for the determination of acrylamide in foods. *Journal of Food Composition and Analysis* **2009**, *22* (2), 142–147.
- (15) Kocadağlı, T.; Gökmen, V. Investigation of alpha-dicarbonyl compounds in baby foods by high-performance liquid chromatography coupled with electrospray ionization mass spectrometry. *J. Agric. Food Chem.* **2014**, *62* (31), 7714–7720.
- (16) Van Boekel, M. A. J. S. Statistical Aspects of Kinetic Modeling for Food Science Problems. *J. Food Sci.* **1996**, *61* (3), 477–486.
- (17) Cämmerer, B.; Kroh, L. W. Shelf life of linseeds and peanuts in relation to roasting. *LWT - Food Science and Technology* **2009**, *42* (2), 545–549.
- (18) Göncüoğlu Taş, N.; Gökmen, V. Maillard reaction and caramelization during hazelnut roasting: A multiresponse kinetic study. *Food Chem.* **2017**, *221*, 1911–1922.
- (19) Batool, Z.; Xu, D.; Wu, M.; Jiao, W.; Roobab, U.; Weng, L.; Zhang, X.; Li, X.; Liang, Y.; Li, B. Determination of α -dicarbonyl compounds and 5-hydroxymethylfurfural in commercially available preserved dried fruits and edible seeds by optimized UHPLC–HR/MS and GC–TQ/MS. *Journal of Food Processing and Preservation* **2020**, *44* (12), 1 DOI: [10.1111/jfpp.14988](https://doi.org/10.1111/jfpp.14988).
- (20) Agila, A.; Barringer, S. Effect of roasting conditions on color and volatile profile including HMF level in sweet almonds (*Prunus dulcis*). *J. Food Sci.* **2012**, *77* (4), C461–468.
- (21) Fallico, B.; Arena, E.; Zappalà, M. Roasting of hazelnuts. Role of oil in colour development and hydroxymethylfurfural formation. *Food Chem.* **2003**, *81* (4), 569–573.
- (22) Ulbricht, R. J.; Northup, S. J.; Thomas, J. A. A Review of 5-Hydroxymethylfurfural (HMF) in Parenteral Solutions. *Toxicol. Sci.* **1984**, *4* (5), 843–853.
- (23) Schlormann, W.; Birringer, M.; Bohm, V.; Lober, K.; Jahreis, G.; Lorkowski, S.; Muller, A. K.; Schone, F.; Gleis, M. Influence of roasting conditions on health-related compounds in different nuts. *Food Chem.* **2015**, *180*, 77–85.
- (24) Zhang, G.; Huang, G.; Xiao, L.; Seiber, J.; Mitchell, A. E. Acrylamide formation in almonds (*Prunus dulcis*): influences of roasting time and temperature, precursors, varietal selection, and storage. *J. Agric. Food Chem.* **2011**, *59* (15), 8225–8232.
- (25) Amrein, T.; Andres, L.; Schönbacher, B.; Conde-Petit, B.; Escher, F.; Amadò, R. Acrylamide in almond products. *European Food Research and Technology* **2005**, *221* (1–2), 14–18.
- (26) Amrein, T.; Lukac, H.; Andres, L.; Perren, R.; Escher, F.; Amadò, R. *Acrylamide in Roasted Almonds and Hazelnuts* **2005**, *53*, 7819.
- (27) Nematollahi, A.; Kamankesh, M.; Hosseini, H.; Hadian, Z.; Ghasemi, J.; Mohammadi, A. Investigation and determination of acrylamide in 24 types of roasted nuts and seeds using micro-extraction method coupled with gas chromatography–mass spec-

trometry: central composite design. *Journal of Food Measurement and Characterization* **2020**, *14* (3), 1249–1260.

(28) Jagerstad, M.; Skog, K. Genotoxicity of heat-processed foods. *Mutat. Res.* **2005**, *574* (1–2), 156–172.

(29) Ölmez, H.; Tuncay, F.; Özcan, N.; Demirel, S. A survey of acrylamide levels in foods from the Turkish market. *Journal of Food Composition and Analysis* **2008**, *21* (7), 564–568.

(30) De Paola, E. L.; Montevecchi, G.; Masino, F.; Garbini, D.; Barbanera, M.; Antonelli, A. Determination of acrylamide in dried fruits and edible seeds using QuEChERS extraction and LC separation with MS detection. *Food Chem.* **2017**, *217*, 191–195.

(31) Brands, C. M. J.; van Boekel, M. Kinetic modeling of reactions in heated monosaccharide-casein systems. *J. Agric. Food Chem.* **2002**, *50*, 6725–6739.

(32) Perez Locas, C.; Yaylayan, V. A. Isotope Labeling Studies on the Formation of 5-(Hydroxymethyl)-2-furaldehyde (HMF) from Sucrose by Pyrolysis-GC/MS. *J. Agric. Food Chem.* **2008**, *56* (15), 6717–6723.

(33) Belitz, H.-D.; Grosch, W.; Schieberle, P. *Food Chemistry*; Springer-Verlag: Berlin Heidelberg, 2009. DOI: 10.1007/978-3-540-69934-7.

(34) Stadler, R. H.; Robert, F.; Riediker, S.; Varga, N.; Davidek, T.; Devaud, S.; Goldmann, T.; Hau, J.; Blank, I. In-Depth Mechanistic Study on the Formation of Acrylamide and Other Vinylogous Compounds by the Maillard Reaction. *J. Agric. Food Chem.* **2004**, *52* (17), 5550–5558.

(35) Weenen, H. Reactive intermediates and carbohydrate fragmentation in Maillard chemistry. *Food Chem.* **1998**, *62* (4), 393–401.

(36) Jadhav, H.; Pedersen, C. M.; Solling, T.; Bols, M. 3-Deoxyglucosone is an intermediate in the formation of furfurals from D-glucose. *ChemSusChem* **2011**, *4* (8), 1049–1051.

(37) Parker, J. K.; Balagiannis, D. P.; Higley, J.; Smith, G.; Wedzicha, B. L.; Mottram, D. S. Kinetic model for the formation of acrylamide during the finish-frying of commercial french fries. *J. Agric. Food Chem.* **2012**, *60* (36), 9321–9331.

(38) Gökmen, V.; Kocadağlı, T.; Göncüoğlu, N.; Mogol, B. A. Model studies on the role of 5-hydroxymethyl-2-furfural in acrylamide formation from asparagine. *Food Chem.* **2012**, *132* (1), 168–174.

(39) Bertuzzi, T.; Martinelli, E.; Mulazzi, A.; Rastelli, S. Acrylamide determination during an industrial roasting process of coffee and the influence of asparagine and low molecular weight sugars. *Food Chem.* **2020**, *303*, 125372.

(40) Nguyen, H. T.; Van der Fels-Klerx, H. J.; Peters, R. J.; Van Boekel, M. A. Acrylamide and 5-hydroxymethylfurfural formation during baking of biscuits: Part I: Effects of sugar type. *Food Chem.* **2016**, *192*, 575–585.

(41) Friedman, M.; Levin, C. E. Review of Methods for the Reduction of Dietary Content and Toxicity of Acrylamide. *J. Agric. Food Chem.* **2008**, *56* (15), 6113–6140.

(42) Knol, J. J.; van Loon, W. A. M.; Linsen, J. P. H.; Ruck, A.-L.; van Boekel, M. A. J. S.; Voragen, A. G. J. Toward a Kinetic Model for Acrylamide Formation in a Glucose–Asparagine Reaction System. *J. Agric. Food Chem.* **2005**, *53* (15), 6133–6139.

(43) Kocadağlı, T.; Göncüoğlu, N.; Hamzaloğlu, A.; Gökmen, V. In depth study of acrylamide formation in coffee during roasting: role of sucrose decomposition and lipid oxidation. *Food Funct* **2012**, *3* (9), 970–975.

(44) De Vleeschouwer, K.; Plancken, I. V. d.; Loey, A. V.; Hendrickx, M. E. Role of precursors on the kinetics of acrylamide formation and elimination under low moisture conditions using a multiresponse approach – Part I: Effect of the type of sugar. *Food Chem.* **2009**, *114* (1), 116–126.